

# Stochastic Dynamic Games in Belief Space

Wilko Schwarting, Alyssa Pierson, Sertac Karaman, and Daniela Rus

**Abstract**—Information gathering while interacting with other agents is critical in many emerging domains, such as self-driving cars, service robots, drone racing, and active surveillance. In these interactions, the interests of agents may be at odds with others, resulting in a non-cooperative dynamic game. Since unveiling one’s own strategy to adversaries is undesirable, each agent must independently predict the other agents’ future actions without communication. In the face of uncertainty from sensor and actuator noise, agents have to gain information over their own state, the states of others, and the environment. They must also consider how their own actions reveal information to others. We formulate this non-cooperative multi-agent planning problem as a stochastic dynamic game. Our solution uses local iterative dynamic programming in the belief space to find a Nash equilibrium of the game. We present three applications: active surveillance, guiding eyes for a blind agent, and autonomous racing. Agents with game-theoretic belief space planning win 44% more races compared to a baseline without game theory and 34% more than without belief space planning.

**Index Terms**—Motion and Path Planning, Optimization and Optimal Control, Multi-Robot Systems, Game-Theoretic Planning

## I. INTRODUCTION

WE aim to develop planners for multi-agent systems that are robust under uncertainty and combine information-seeking behavior with game-theoretic reasoning. While game theory can model the interaction and dependency among agents, it does not address the quality of information available to the agent for decision making. Agents must plan and act within a game, gain information, and leverage the information gain to improve their control policies. We propose an approach that combines game-theoretic planning with belief-space planning, leveraging the interaction models from game theory while incorporating uncertainties in the perception.

In multi-agent systems, we find that agents gather information to reduce uncertainty while maintaining decision-making strategies that support complex interactions. While each agent operates independently, they have a model of what the other agents are or should be doing. This model can be prescribed, observed, sensed, or communicated. Applications include assistive robotics, surveillance, pursuer-evader games, and racing.

This work is supported in part by NSF Grant 1723943, the Office of Naval Research (ONR) Grant N00014-18-1-2830, and Toyota Research Institute (TRI). TRI provided funds to assist the authors with their research but this article solely reflects the opinions and conclusions of its authors and not TRI or any other Toyota entity. (Corresponding author: Wilko Schwarting.)

W. Schwarting, A. Pierson, and D. Rus are with the Computer Science and Artificial Intelligence Laboratory (CSAIL), Massachusetts Institute of Technology, Cambridge, MA 02139 USA (e-mail: {wilkos, apierson, rus}@csail.mit.edu).

S. Karaman is with the Laboratory of Information and Decision Systems (LIDS), Massachusetts Institute of Technology, Cambridge, MA 02139 USA (e-mail: sertac@mit.edu).

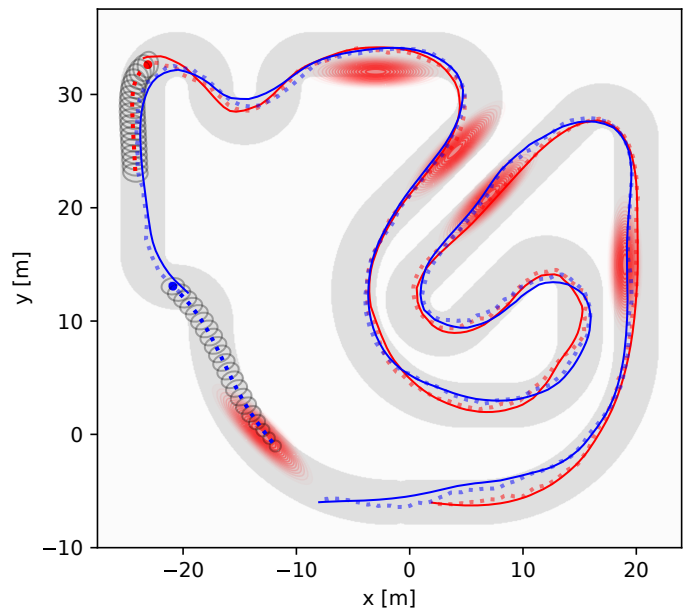


Fig. 1. One application we present is dynamic racing. Here, the blue agent starts with a disadvantage, but is equipped with better acceleration and capable of moving faster through corners than the red agent. Our approach allows the blue agent to overtake and win the race. Planned trajectories and chance constraints are shown in dashed lines and ellipses. The traces correspond to the true state (solid) and the noisy EKF-estimate (dashed) available to each agent during the race. The red areas are zones with low noise observations and reduce uncertainty.

Within the game-theoretic framework, agents take actions that increase their information gain, which in turn results in the ability to improve their control policies with reduced uncertainty. For example, an assistive robot tasked with guiding a human may explore the environment to reduce uncertainty and better navigate. Conversely, a game-theoretic setting can model adversarial agents. Here, agents may choose to “hide” to prevent others from gathering information about themselves, which is relevant to surveillance applications. In the context of racing, agents may force others to increase their uncertainty, such as by pressuring them to drive too fast in a corner which increases uncertainty in their state, or by simply pushing them into the dark. It is therefore not only important to reason about a robot’s own uncertainty but also the uncertainty of other agents in the environment, and even more so how one’s actions impact the change in uncertainty of others.

Game-theoretic models have not only proven useful to model interactions between autonomous systems, but also in integrating interactive human predictions into autonomous decision-making and planning. We can model the actions of humans as expected cost-minimizing and estimate human cost functions from past observed trajectories with Inverse

Reinforcement Learning (IRL) [1]. Consequently, computing expected cost-minimizing actions based on the learned cost functions generates human predictions. The expected cost-minimizing behavior can also be interpreted as a best response to an autonomous agent’s actions. This best response setting allows us to estimate how the autonomous system’s actions influence human actions. The autonomous system can therefore indirectly control the human’s actions to a certain degree. This technique has been applied to predict human behavior for autonomous vehicles [2, 3], and to predict pedestrians [4]. The combination of game-theoretic modeling of human behavior and information seeking planning are therefore even more promising.

Home service robots can provide assistance and support to humans, particularly the elderly population. These robots need to work in close proximity of humans, gauge the human’s intent, and understand the state of mind of others to better perform tasks. They have to avoid confusion and misunderstandings and will need to seek information about both their environment and surrounding humans. Additionally, these autonomous systems need to also reason about the amount of information and understanding the human has about the robot. The robot can aid the human’s understanding through explicit communication, as well as implicitly through behavior, such as moving to visible locations or clearly indicating intent by unambiguously moving in a desired direction.

We propose a solution that combines multi-agent game-theoretic decision-making under uncertainty and belief space planning (BSP). Our approach supports robust solutions to a wide range of multi-robot applications where dealing with uncertainty, the need to gather information, and game-theoretic decision-making are fundamental. We build on important advancements in two areas: game-theoretic planning and belief space planning. Game-theoretic planning successfully solves problems where an agent’s objective is at odds with the objective of other agents, such as in modeling human behavior in traffic [5, 6, 7], and leveraging the effects on humans by autonomous cars [2]. A recent review on game theory and control can be found in [8]. In game theory, the Nash equilibrium is a proposed solution of a non-cooperative game involving two or more players. Each player is assumed to know the equilibrium strategies of the other players, and no player has anything to gain by changing only their own strategy. Solving for Nash equilibria has been applied to competitive racing [9, 10, 11] and guiding vehicles through intersections [12]. Solution methods in racing include Iterated Best Response [9, 11], using discrete payoff matrices [10], or solving the necessary conditions. We will solve for the necessary condition at each stage in the backward-pass of iterative dynamic programming to iteratively solve for the Nash equilibrium of the game.

While game-theoretic planning models the interaction and dependency among agents, it does not address the quality of information available to the agent for decision making. Belief-space planning [13] uses beliefs, which are the distributions of the robot’s state estimate, to represent the uncertainties in the perception of the robot. The problem of computing a control

policy over the space of belief states is formally described as a Partially Observable Markov Decision Process (POMDP), and has been studied extensively. Solutions to POMDPs are known to be very complex. Solving a POMDP to global optimality is NP-hard: solutions such as point-based algorithms [14, 15, 16, 17] in discrete space are bound to the curse of history, as well as sampling based solvers [18, 19, 20]. Optimization-based approaches have been developed for planning in continuous belief space [21, 22, 23, 24, 25], by approximating beliefs as Gaussian distributions and computing a value function valid in local regions of the belief space. In comparison to point-based algorithms which scale exponentially in the planning horizon  $l$ , optimization-based methods scale linearly,  $\mathcal{O}(l)$ . We follow this direction but do not rely on the common maximum-likelihood observation assumption [23, 22].

The cognitive theory of mind [26] is separated into first-order belief space (e.g., I think they think that...) and second-order belief space (e.g., I think they think that I think that...), essentially a belief space over the deduced belief space of others. In general one can imagine higher order belief spaces since one can continue this chain of reasoning infinitely often (e.g., I think they think that I think they think that I think... and so on). Formulating beliefs over beliefs becomes intractable for real-time applications with this infinite recursion. We find that parametrizing belief spaces efficiently is essential to generating real-time capable algorithms. To limit computational complexity, we consider a first-order belief space.

**Assumption 1. First-Order Belief Space:** *We use a first-order approximation of the belief space.*

Under Assumption 1, we limit the recursion in calculating the belief space, which keeps computation complexity at a reasonable level and avoids an explosion in parameters in the recursive beliefs over beliefs. In Section IV, we evaluate cases, such as competitive racing, where this assumption is a simplification of the true system dynamics. In the racing game, all agents reason about themselves and also have a belief over others, but do not reason about the belief others have about themselves. The first-order belief assumption states that agents A’s belief over agent B is the same as agent B’s belief about themselves, which is not necessarily the case in the real world. However, while these belief mismatches may occur, we see performance improvements over a game-theoretic baseline without belief space planning, see Sec. IV-C, which highlights the importance of accounting for uncertainty and information gain in competitive racing and other applications.

The first order belief assumption implies “common knowledge” of costs, dynamics, and measurement functions for all agents. Assumption 2 defines this shared knowledge among the agents.

**Assumption 2. Cost, dynamics, and observation functions of each agent are known by every agent, such that each agent can predict the actions of other agents using these functions.**

Similar assumptions have been made by related game-theoretic works, see [2, 5, 9, 10, 11]. Note that Assumption 2 only states that agents share knowledge of the functions, but

each agent still performs its individual computation of these values with its own noise.

We present a computationally-tractable solution to multi-agent planning that combines game-theoretic planning and belief space planning to interact within a problem formulated as a game, gain information, and leverage the information gain to improve the agents' control policies. The main limiting factor in applying either game theory or belief space planning, and even more so the combination of both to robotic control problems lies in the associated computational complexity. To the best of our knowledge this is the first work to combine general dynamic games and planning in belief space into an efficient real-time algorithm. The main contributions of this paper are:

- 1) A method for computing Nash equilibria for dynamic games in belief space;
- 2) A linear feedback law, similar to linear-quadratic Gaussian control (LQG) for the robot resulting from the solution, and also a predicted linear feedback law for all other agents;
- 3) State and control trajectory based regularization to ensure convergence;
- 4) Evaluation of the proposed method in three stochastic dynamic games: racing with autonomous vehicles, active surveillance, and guiding eyes for a blind agent.

The remainder of the paper is organized as follows: Section II introduces dynamic games in belief space, including a general definition of best response POMDPs and a Nash equilibrium formulation of the non-cooperative dynamic game. The resulting problem definition is given in Section II-A, and assuming beliefs can be represented in the form of Gaussian distributions, approximating the belief dynamics based on an extended Kalman filter is detailed in Section III-A. Our method computes a locally-optimal solution to the best response POMDP problem with continuous state and action spaces and non-linear dynamics and observation models by iteratively solving for a local Nash equilibrium, outlined in Section III. We utilize a belief space variant of iterative linear-quadratic Gaussian control (iLQG) to compute the Nash equilibrium, Section III-C, by solving for a local Nash equilibrium at each stage of the backward pass, see Section III-B. At each iteration, each agent's value function is approximated based on a quadratization around a nominal trajectory, and the belief dynamics are approximated with an extended Kalman filter. We describe regularization techniques in Section III-D to ensure that the algorithm converges regardless of initial conditions. Based on these findings, we introduce Algorithm 1 in Section III-E describing the full belief space Nash equilibrium computation.

We show the potential of our approach in Section IV by presenting three multi-agent problems that combine the information-seeking behavior with our game-theoretic formulation: active surveillance, guiding blind agents, and racing with autonomous vehicles.

## II. DYNAMIC GAMES IN BELIEF SPACE

We first define POMDPs in their most general form (following notation of [27, 24]), then formulate the resulting game

TABLE I  
MAIN SYMBOLS AND NOTATION

$\mathbf{x}, \mathbf{u}, \mathbf{z}, \mathbf{b}$	State, control input, and measurement
$\mathbf{b}, \mathbf{s} = [\mathbf{b}^\top, \mathbf{u}^\top]^\top$	Belief, short for belief and controls
$Q^i, V^i$	Action-value and value function of agent $i$
$\pi^i$	Optimal control policy of agent $i$
$j_k, K_k$	feedforward and feedback gains at time $k$
$c_k^i(\mathbf{b}_k, \mathbf{u}_k), c_i^i(\mathbf{b}_i)$	Cost of agent $i$ at time $k$ , and terminal cost
$\mathbf{x}_{k+1} = f(\mathbf{x}_k, \mathbf{u}_k, \mathbf{m}_k)$	State transition with process noise $\mathbf{m}_k$
$\mathbf{z}_k = h(\mathbf{x}_k, \mathbf{n}_k)$	Measurement function with meas. noise $\mathbf{n}_k$
$\mathbf{b}_{k+1} = \beta(\mathbf{b}_k, \mathbf{u}_k, \mathbf{z}_{k+1})$	Belief transition
$\mathbf{b} = \bar{\mathbf{b}} + \delta \mathbf{b}$	Nominal + perturbation, similar for $\mathbf{u}, \mathbf{s}$
$c_{\mathbf{s},k}^i, c_{\mathbf{ss},k}^i$	Jacobian and Hessian of $c_k^i$ evaluated at $\bar{\mathbf{s}}_k$
	Similar for other partial derivatives

and derive the Nash Equilibrium to be solved for.

We write the belief space planning problem as a stochastic optimal control problem. Consider a system of  $N$  agents  $i \in \{1, \dots, N\}$ , with agent  $i$ 's state at time  $k$  denoted  $\mathbf{x}_k^i \in \mathbb{R}^{n_{x^i}}$ , measurement as  $\mathbf{z}_k^i \in \mathbb{R}^{n_{z^i}}$ , and control input  $\mathbf{u}_k^i \in \mathbb{R}^{n_{u^i}}$ . For brevity we refer to  $\mathbf{x}_k = [\mathbf{x}_k^{1,\top}, \dots, \mathbf{x}_k^{N,\top}]^\top \in \mathbb{R}^{n_x}$  as the joint state,  $\mathbf{z}_k = [\mathbf{z}_k^{1,\top}, \dots, \mathbf{z}_k^{N,\top}]^\top \in \mathbb{R}^{n_z}$  as the joint measurement, and  $\mathbf{u}_k = [\mathbf{u}_k^{1,\top}, \dots, \mathbf{u}_k^{N,\top}]^\top \in \mathbb{R}^{n_u}$  as the joint control, consisting of all agents, and  $\mathbf{u}_k^{-i}$  indicates controls of all other agents except  $i$ . We will refer to  $\mathbf{u} = [\mathbf{u}_0, \mathbf{u}_1, \dots, \mathbf{u}_{l-1}]$  as the control trajectory until time  $l$ . Let  $\mathbf{b}^{ij}$  be the individual belief about the  $i$ -th agent computed by the  $j$ -th agent. By applying Assumption 1, we have that  $\mathbf{b}^{ij} \approx \mathbf{b}^{ii}$ , or in other words agent  $j$ 's belief over agent  $i$  is the same as agent  $i$ 's belief about themselves. Thus, we will just use the notation  $\mathbf{b}^i$  to refer to the individual belief about the  $i$ -th agent. The joint *belief*  $\mathbf{b}(\mathbf{x}_k)$  is defined as the distribution of the state  $\mathbf{x}_k$  given all past control inputs and sensor measurements, and consists of individual beliefs  $\mathbf{b}^i$ . For brevity, we define  $\mathbf{s} = [\mathbf{b}^\top, \mathbf{u}^\top]^\top$ .

Following [27, 24], we compute the belief by

$$\mathbf{b}(\mathbf{x}_k) = p(\mathbf{x}_k | \mathbf{u}_0, \dots, \mathbf{u}_{k-1}, \mathbf{z}_1, \dots, \mathbf{z}_k), \quad (1)$$

from all past control inputs and sensor measurements. The stochastic dynamics and observation model, here formulated in probabilistic notation as

$$\mathbf{x}_{k+1} \sim p(\mathbf{x}_{k+1} | \mathbf{x}_k, \mathbf{u}_k), \quad \mathbf{z}_k \sim p(\mathbf{z}_k | \mathbf{x}_k), \quad (2)$$

can be used to propagate the belief given a control input  $\mathbf{u}_k$  and a measurement  $\mathbf{z}_{k+1}$  by Bayesian filtering:

$$\mathbf{b}(\mathbf{x}_{k+1}) = \eta p(\mathbf{z}_{k+1} | \mathbf{x}_{k+1}) \int p(\mathbf{x}_{k+1} | \mathbf{x}_k, \mathbf{u}_k) \mathbf{b}(\mathbf{x}_k) d\mathbf{x}_k. \quad (3)$$

In (3),  $\eta$  is a normalizer independent of  $\mathbf{x}_{k+1}$  and  $\mathbf{b}(\mathbf{x}_{k+1})$  contains the uncertainty originating from the stochastic dynamics, the uncertain measurement and the uncertainty in the belief at the previous time step. We employ the shorthand  $\mathbf{b}_k$  to refer to  $\mathbf{b}(\mathbf{x}_k)$ . The stochastic *belief dynamics* are defined by (3) and are written as

$$\mathbf{b}_{k+1} = \beta(\mathbf{b}_k, \mathbf{u}_k, \mathbf{z}_{k+1}). \quad (4)$$

The expected return of each individual agent  $i$  under a control trajectory of all agents  $\mathbf{u}$ , including its own control

trajectory  $\mathbf{u}^i$ , subject to uncertainty on the observed measurements  $\mathbf{z}$  over the horizon  $l$  is determined by the action-value function

$$Q^i(\mathbf{b}_0, \mathbf{u}) = \mathbb{E}_{\mathbf{z}} \left[ c_l^i(\mathbf{b}_l) + \sum_{k=0}^{l-1} c_k^i(\mathbf{b}_k, \mathbf{u}_k) \right]. \quad (5)$$

Here  $c_k^i(\cdot)$  denotes the cost at time  $k$  and  $c_l^i(\cdot)$  denotes the terminal cost of agent  $i$ . Since there exists an action-value function for each agent, there are  $N$  distinct action-value functions  $Q^i$  for  $i \in \{1, \dots, N\}$ .

We will first formulate the two problems of (1) solving the general POMDP best response game, and then (2) finding the Nash equilibrium of this game.

**Problem 1. POMDP Best Response Game:** *Given an initial belief  $\mathbf{b}_0$ , for agents  $i \in \{1, \dots, N\}$ , we need to solve the stochastic optimal control problem*

$$\pi^i(\mathbf{b}_0) = \arg \min_{\mathbf{u}^i} Q^i(\mathbf{b}_0, \mathbf{u}) \quad \forall i \in \{1, \dots, N\} \quad (6)$$

$$s.t. \mathbf{b}_{k+1} = \beta(\mathbf{b}_k, \mathbf{u}_k, \mathbf{z}_{k+1}), \quad (7)$$

for each agent by minimizing each agent's expected cost with respect to their own controls  $\mathbf{u}^i$ , where  $Q^i(\mathbf{b}_0, \mathbf{u})$  is the action-value function of agent  $i$ .

Note that all agents' optimal policies  $\pi^i(\mathbf{b}_0, \mathbf{u}^{-i})$  depend on the actions of all other agents because each agent  $i$  minimizes their own action-value function  $Q^i(\mathbf{b}_0, \mathbf{u})$ . The result is a non-cooperative game [28] in which all agents' policies depend on the optimal policies of all other agents  $\pi^i(\mathbf{b}_0, \pi^{-i})$ . Since all policies are optimized jointly and severally, the dependence of agent  $i$ 's policy  $\pi^i$  on other agents' controls  $\mathbf{u}^{-i}$  is resolved by inserting their optimal policy  $\pi^{-i}$ . We therefore denote  $\pi^i(\mathbf{b}_0)$  instead of  $\pi^i(\mathbf{b}_0, \mathbf{u}^{-i})$ .

A general solution to (6) can be defined recursively by the Bellman equation:

$$V_l^i(\mathbf{b}_l) = c_l(\mathbf{b}_l), \quad (8)$$

$$Q_k^i(\mathbf{b}_k, \mathbf{u}_k) = c_k^i(\mathbf{b}_k, \mathbf{u}_k) + \mathbb{E}_{\mathbf{z}_{k+1}} [V_{k+1}^i(\beta(\mathbf{b}_k, \mathbf{u}_k, \mathbf{z}_{k+1}))],$$

$$V_k^i(\mathbf{b}_k) = \min_{\mathbf{u}_k^i} Q_k^i(\mathbf{b}_k, \mathbf{u}_k),$$

$$\pi_k^i(\mathbf{b}_k) = \arg \min_{\mathbf{u}_k^i} Q_k^i(\mathbf{b}_k, \mathbf{u}_k),$$

where  $V_k^i(\mathbf{b}_k)$  is the value function and  $\pi_k^i(\mathbf{b}_k)$  the optimal policy at time  $k$ . Note that in (8) the cost  $c_k^i(\mathbf{b}_k, \mathbf{u}_k)$ , the reached value function  $V_{k+1}^i(\beta(\mathbf{b}_k, \mathbf{u}_k, \mathbf{z}_{k+1}))$ , and therefore the action-value function  $Q_k^i(\mathbf{b}_k, \mathbf{u}_k)$  of agent  $i$  depends not only on its own action but also on all other players' actions. This interdependence is analogous to (6) but formulated recursively over time.

More precisely, the interdependence of all players optimal policies is captured in the Nash equilibrium of Problem 1, defined in Problem 2.

**Problem 2. Nash Equilibrium:** *Find the optimal control policy  $\pi = [\pi^1, \dots, \pi^N]^T$  that yields a local Nash*

*equilibrium of the POMDP Best Response Game in Problem 1, such that it satisfies*

$$Q^i(\mathbf{b}_0, \mathbf{u}^i, \pi^{-i}) \geq Q^i(\mathbf{b}_0, \pi^i, \pi^{-i}), \forall i \in \{1, 2, \dots, N\}, \quad (9)$$

for all  $\mathbf{u}^i$  in the neighborhood of  $\pi^i$ .

Based on the necessary condition of Problem 2, we will derive a local necessary condition for each sub-problem in the backward pass of our game-theoretic variant of belief iLQG.

### A. Problem Formulation

The difficulty in solving POMDPs stems from the infinite-dimensional space of all beliefs, and that in general the value function cannot be expressed in parametric form. To overcome these challenges we describe beliefs by Gaussian distributions, approximating the belief dynamics using an extended Kalman filter, and a quadratic approximation of the value function about a nominal trajectory through the belief space. We iteratively compute a local Nash equilibrium over all agents in the proximity of the nominal trajectory by solving the necessary condition (9) of Problem 2 at each timestep during a belief-space variant of iLQG to perform the Bellman backwards recursion in (8). Due to its similarity to iLQG we benefit from linear scaling  $\mathcal{O}(l)$  in the planning horizon  $l$ , in contrast to point-based POMDP algorithms which scale exponentially.

We are given non-linear stochastic dynamics and observation models in state-transition notation:

$$\mathbf{x}_{k+1} = f(\mathbf{x}_k, \mathbf{u}_k, \mathbf{m}_k), \quad \mathbf{m}_k \sim \mathcal{N}(0, I), \quad (10)$$

$$\mathbf{z}_k = h(\mathbf{x}_k, \mathbf{n}_k) \quad \mathbf{n}_k \sim \mathcal{N}(0, I), \quad (11)$$

where  $\mathbf{m}_k$  and  $\mathbf{n}_k$  are the motion and measurement noise, respectively. Without loss of generality, we draw both the motion and measurement noise from independent Gaussian distributions with zero mean and unit variance since the noise can be arbitrarily transformed inside these functions. Depending on the system, motion and sensing noise may be state and control dependent.

Note that formulating the general dynamics and measurement functions jointly of all agents includes, but is not limited to, the special case of independent functions for each agent  $i$  as in

$$f(\mathbf{x}_k, \mathbf{u}_k, \mathbf{m}_k) = [f^1(\mathbf{x}_k^1, \mathbf{u}_k^1, \mathbf{m}_k^1)^T, \dots, f^N(\mathbf{x}_k^N, \mathbf{u}_k^N, \mathbf{m}_k^N)^T]^T, \quad (12)$$

$$h(\mathbf{x}_k, \mathbf{n}_k) = [h^1(\mathbf{x}_k^1, \mathbf{n}_k^1)^T, \dots, h^N(\mathbf{x}_k^N, \mathbf{n}_k^N)^T]^T. \quad (13)$$

We define the Gaussian belief as  $\mathbf{b}_k = (\hat{\mathbf{x}}_k^T, \Sigma_k)$ , by the mean state  $\hat{\mathbf{x}}_k$  and the variance  $\Sigma_k$  of the Normal distribution  $\mathcal{N}(\hat{\mathbf{x}}_k, \Sigma_k)$ .

## III. TECHNICAL APPROACH

Before detailing the value iteration method for the Nash equilibrium solution based on a belief-space variant of iLQG in Section III-C, we need to derive two important components. First, we describe the approximation of the general Bayesian

filter update (4) by an EKF in Section III-A to formulate the gaussian belief dynamics. This allows us to forward propagate Gaussian beliefs given an initial belief and a control trajectory which we utilize in the game-theoretic variant of belief space iLQG. Second, we show that the necessary condition of Problem 2, the Nash equilibrium, is equivalent to a local necessary condition at each timestep in the Bellman recursion in Section III-B. The full algorithm is detailed in Section III-E.

### A. Bayesian Filter and Belief Dynamics

The general belief dynamics of a current belief  $\mathbf{b}_k$  and measurement  $\mathbf{z}_{k+1}$  are given by the Bayesian filter in (4). To make the belief propagation tractable we follow [29] and approximate the Bayesian filter by an extended Kalman filter (EKF), suitable for non-linear Gaussian beliefs. For well-defined transition models, the EKF is the standard for nonlinear state estimation [30, 31]. The EKF makes a first-order approximation of  $f(\mathbf{x})$  with respect to the stochastic variable  $\mathbf{x}$ , such that for a given belief  $\mathbf{b}_k = (\hat{\mathbf{x}}_k, \Sigma_k)$  we have the standard EKF update equations [24, 27]

$$\begin{aligned}\hat{\mathbf{x}}_{k+1} &= f(\hat{\mathbf{x}}_k, \mathbf{u}_k, 0) + K_k(\mathbf{z}_{k+1} - h(f(\hat{\mathbf{x}}_k, \mathbf{u}_k, 0), 0)), \\ \Sigma_{k+1} &= \Gamma_{k+1} - K_k H_k \Gamma_{k+1},\end{aligned}\quad (14)$$

with corresponding matrices defined by

$$\begin{aligned}\Gamma_{k+1} &= A_k \Sigma_k A_k^T + M_k M_k^T, \\ K_k &= \Gamma_{k+1} H_k^T (H_k \Gamma_{k+1} H_k^T + N_k N_k^T)^{-1}, \\ A_k &= \frac{\partial f}{\partial \mathbf{x}}(\hat{\mathbf{x}}_k, \mathbf{u}_k, 0), \quad M_k = \frac{\partial f}{\partial \mathbf{m}}(\hat{\mathbf{x}}_k, \mathbf{u}_k, 0), \\ H_k &= \frac{\partial h}{\partial \mathbf{x}}(f(\hat{\mathbf{x}}_k, \mathbf{u}_k, 0), 0), \quad N_k = \frac{\partial h}{\partial \mathbf{n}}(f(\hat{\mathbf{x}}_k, \mathbf{u}_k, 0), 0).\end{aligned}\quad (15)$$

The belief update is dependent on the noisy measurement  $\mathbf{z}_k$ , causing the belief dynamics to be stochastic. We define  $\mathbf{b}_k = [\hat{\mathbf{x}}_k^T, \text{vec}(\Sigma_k)^T]^T$ , where  $\text{vec}(\Sigma_k)$  is the matrix  $\Sigma_k$  reshaped into vector form, and formulate the stochastic belief dynamics

$$\mathbf{b}_{k+1} = g(\mathbf{b}_k, \mathbf{u}_k) + W(\mathbf{b}_k, \mathbf{u}_k) \xi_k, \quad \xi_k \sim \mathcal{N}(0, I), \quad (16)$$

where  $\xi_k$  is a Gaussian with dimension of the state  $n_x$  and

$$g(\mathbf{b}_k, \mathbf{u}_k) = \begin{bmatrix} f(\hat{\mathbf{x}}_k, \mathbf{u}_k, 0) \\ \text{vec}(\Gamma_{k+1} - K_k H_k \Gamma_{k+1}) \end{bmatrix}, \quad (17)$$

$$W_k(\mathbf{b}_k, \mathbf{u}_k) = \begin{bmatrix} \sqrt{K_k H_k \Gamma_{k+1}} \\ \mathbf{0} \end{bmatrix}. \quad (18)$$

In this form  $\xi_k$  represents both measurement-  $\mathbf{n}_k$  and motion noise  $\mathbf{m}_k$  mapped onto the belief transition. The stochastic Gaussian belief dynamics allow us to propagate beliefs efficiently during the forward pass of the game-theoretic variant of belief space iLQG.

### B. Nash Equilibrium Necessary Condition

While formulating how to propagate uncertainty for the continuous POMDP, we also need to define a tractable procedure to solve for Nash equilibria. One common method to solve for Nash equilibria is the method of Iterated Best Response [9, 11], where control policies are exchanged after

each agent's separate and independent optimization iteration. In contrast, we directly integrate the necessary condition of the Nash equilibrium into the backward pass of a belief space variant of iLQG. Specifically, we solve a quadratic game at each stage of the backward pass with a unique solution. First, we formulate the necessary condition of Problem 2 as

$$\frac{\partial Q^i(\mathbf{u})}{\partial \mathbf{u}^i} = 0, \quad \forall i \in \{1, 2, \dots, N\}, \quad (19)$$

which allows us to compute local Nash equilibria by solving (19). Theorem 1 states an equivalent condition for  $Q_k^i(\mathbf{b}_k, \mathbf{u}_k)$ , the expected cost-to-go function from time  $k$  to  $l$ , defined in the Bellman recursion (8).

**Theorem 1.** *The necessary condition of the local Nash equilibrium (19) is equivalent to*

$$\frac{\partial Q_k^i(\mathbf{b}_k, \mathbf{u}_k)}{\partial \mathbf{u}_k^i} = 0, \quad (20)$$

for all  $i \in \{1, 2, \dots, N\}$ , and  $k \in \{0, 1, \dots, l-1\}$ .

*Proof:* The proof of Theorem 1 follows from the backward recursion in (8). Starting from time  $(l-1)$  we see that  $\frac{\partial Q_{l-1}^i(\mathbf{b}_{l-1}, \mathbf{u}_{l-1})}{\partial \mathbf{u}_{l-1}^i} = \frac{\partial Q^i(\mathbf{b}, \mathbf{u})}{\partial \mathbf{u}^i} = 0$ , since the expected costs at previous time steps are unaffected by  $\mathbf{u}_{l-1}^i$ . With the same argument and following the Bellman recursion backwards in time we find that  $\left[ \frac{\partial Q^i(\mathbf{b}, \mathbf{u})}{\partial \mathbf{u}_{l-1}^i}, \frac{\partial Q^i(\mathbf{b}, \mathbf{u})}{\partial \mathbf{u}_{l-2}^i}, \dots, \frac{\partial Q^i(\mathbf{b}, \mathbf{u})}{\partial \mathbf{u}_k^i} \right]^T = 0$ , is equivalent to

$$\left[ \frac{\partial Q_{l-1}^i(\mathbf{b}_{l-1}, \mathbf{u}_{l-1})}{\partial \mathbf{u}_{l-1}^i}, \dots, \frac{\partial Q_k^i(\mathbf{b}_k, \mathbf{u}_k)}{\partial \mathbf{u}_k^i} \right]^T = 0,$$

for  $k \leq l-1$ . By this reasoning,  $Q_k^i(\mathbf{b}_k, \mathbf{u}_k)$  only depends on the subsequent controls, thus completing the proof. ■

Furthermore, if each agent  $i$  finds a policy  $\pi_k^i$  to the Bellman recursion, all  $\frac{\partial Q_k^i(\mathbf{b}_k, \mathbf{u}_k)}{\partial \mathbf{u}_k^i} = 0$  necessary conditions are fulfilled at time  $k$ . Note that each agents' policy  $\pi^i(\mathbf{u}^{-i})$  depends on the other agents' inputs  $\mathbf{u}^{-i}$ , where  $-i$  indicates all other agents. Therefore, solving the Bellman recursion simultaneously for all agents defines a static game [28], but more so a game at each stage  $k$  of the backward-pass.

In the next section, we describe our solution for integrating the Nash equilibrium necessary condition at every time  $k$  into the backward pass of a belief-space variant of iLQG.

### C. Iterative Dynamic Programming

In this section we describe our belief-space variant of iLQG for computing local Nash equilibria by solving the Bellman recursion defined in (8). We denote the nominal belief as  $\bar{\mathbf{b}} = \mathbf{b} - \delta \mathbf{b}$ , and the nominal controls  $\bar{\mathbf{u}} = \mathbf{u} - \delta \mathbf{u}$ , with  $\bar{\mathbf{s}} = [\bar{\mathbf{b}}^T, \bar{\mathbf{u}}^T]^T$ . At each iteration, the algorithm performs a backward pass and a forward pass on the current estimate of the belief  $\bar{\mathbf{b}} = [\bar{\mathbf{b}}_0, \bar{\mathbf{b}}_1, \dots, \bar{\mathbf{b}}_l]$  and control trajectory  $\bar{\mathbf{u}} = [\bar{\mathbf{u}}_0, \bar{\mathbf{u}}_1, \dots, \bar{\mathbf{u}}_{l-1}]$ , i.e. the nominal trajectories. In the backward pass, the algorithm approximates the value functions for each agent as a quadratic function along the nominal trajectory, and the value function is propagated backwards in

time. In the forward pass we produce a new nominal trajectory based on the value function computed in the backward pass and applying the associated feedback policy. This iterative process continues towards a locally optimal solution to the Nash equilibrium in belief space. The key idea is to maintain a quadratic approximation of  $Q_k^i(\mathbf{b}_k, \mathbf{u}_k)$  and the value functions  $V_k^i(\mathbf{b}_k)$ .

We first derive the quadratic form of  $Q_k^i(\mathbf{b}_k, \mathbf{u}_k)$  in Theorem 2 by a Taylor expansion of the dynamics and costs, then find the minimizing control policy  $\pi_k = [\pi_k^{1,\top}, \dots, \pi_k^{N,\top}]^\top$  by solving the static game and computing the Nash equilibrium over all agents. From this result we compute the value functions  $V_k^i(\mathbf{b}_k) = Q_k^i(\mathbf{b}_k, \pi_k)$  and derive an update law for  $V$  backwards in time.

**Theorem 2.** *By linear expansion of the belief dynamics and quadratic expansion of the cost and value function,  $Q_k^i(\mathbf{s}_k)$  is a quadratic of the form*

$$Q_k^i(\bar{\mathbf{s}}_k + \delta \mathbf{s}_k) \approx Q_k^i + Q_{\mathbf{s},k}^{i,\top} \delta \mathbf{s}_k + \frac{1}{2} \delta \mathbf{s}_k^\top Q_{\mathbf{ss},k}^i \delta \mathbf{s}_k, \quad (21)$$

where

$$Q_k^i = c_k^i + V_{k+1}^i + \frac{1}{2} \sum_{j=1}^{n_x} W_k^{(j),\top} V_{\mathbf{bb},k+1}^i V_{\mathbf{s},k}^{(j)}, \quad (22)$$

$$Q_{\mathbf{s},k}^i = c_{\mathbf{s},k}^i + g_{\mathbf{s},k}^\top V_{\mathbf{b},k+1}^i + \sum_{j=1}^{n_x} W_{\mathbf{s},k}^{(j),\top} V_{\mathbf{bb},k+1}^i W_k^{(j)}, \quad (23)$$

$$Q_{\mathbf{ss},k}^i = c_{\mathbf{ss},k}^i + g_{\mathbf{s},k}^\top V_{\mathbf{bb},k+1}^i g_{\mathbf{s},k} + \sum_{j=1}^{n_x} W_{\mathbf{s},k}^{(j),\top} V_{\mathbf{bb},k+1}^i W_{\mathbf{s},k}^{(j)}. \quad (24)$$

*Proof:* We start by expanding the terms of the action-value function of the Bellman recursion, cf. (8),

$$Q_k^i(\mathbf{b}_k, \mathbf{u}_k) = c_k^i(\mathbf{b}_k, \mathbf{u}_k) + \mathbb{E}_{\xi_k} [V_{k+1}^i(g_k(\mathbf{b}_k, \mathbf{u}_k) + W_k(\mathbf{b}_k, \mathbf{u}_k)\xi_k)], \quad (25)$$

to second order around the nominal control and belief  $\bar{\mathbf{s}}_k = [\bar{\mathbf{b}}_k^\top, \bar{\mathbf{u}}_k^\top]^\top$ . The term  $c_k^i(\mathbf{b}_k, \mathbf{u}_k)$  becomes

$$c_k^i(\bar{\mathbf{s}}_k + \delta \mathbf{s}_k) \approx c_k^i + c_{\mathbf{s},k}^{i,\top} \delta \mathbf{s}_k + \frac{1}{2} \delta \mathbf{s}_k^\top c_{\mathbf{ss},k}^i \delta \mathbf{s}_k, \quad (26)$$

with  $c_k^i = c_k^i(\bar{\mathbf{s}})$ , where  $c_{\mathbf{s},k}^i$  and  $c_{\mathbf{ss},k}^i$  are the Jacobian and Hessian of  $c_k^i$  evaluated at  $\bar{\mathbf{s}}_k$ . To expand the second term on the right hands side of (25) we first expand the stochastic joint belief dynamics to

$$g_k(\bar{\mathbf{s}}_k + \delta \mathbf{s}_k) \approx g_k + g_{\mathbf{s},k} \delta \mathbf{s}_k, \quad (27)$$

$$W_k^{(j)}(\bar{\mathbf{s}}_k + \delta \mathbf{s}_k) \approx W_k^{(j)} + W_{\mathbf{s},k}^{(j)} \delta \mathbf{s}_k, \quad (28)$$

with terms  $g_k = g_k(\bar{\mathbf{s}}_k)$ ,  $W_k^{(j)} = W_k^{(j)}(\bar{\mathbf{s}}_k)$ , and  $g_{\mathbf{s},k}$ ,  $W_{\mathbf{s},k}^{(j)}$  the respective Jacobians evaluated at  $\bar{\mathbf{s}}_k$ .  $W_k^{(j)}$  denotes the  $j$ -th column of matrix  $W_k$ .

We now formulate the second term of (25). We define the value function as a quadratic around  $\bar{\mathbf{b}}_{k+1}$

$$V_{k+1}^i(\bar{\mathbf{b}}_{k+1} + \delta \mathbf{b}_{k+1}) \quad (29)$$

$$\begin{aligned} &\approx V_{k+1}^i + V_{\mathbf{b},k+1}^{i,\top} \delta \mathbf{b}_{k+1} + \frac{1}{2} \delta \mathbf{b}_{k+1}^\top V_{\mathbf{bb},k+1}^i \delta \mathbf{b}_{k+1} \\ &= V_{k+1}^i + V_{\mathbf{b},k+1}^{i,\top} (\mathbf{b}_{k+1} - \bar{\mathbf{b}}_{k+1}) \\ &\quad + \frac{1}{2} (\mathbf{b}_{k+1} - \bar{\mathbf{b}}_{k+1})^\top V_{\mathbf{bb},k+1}^i (\mathbf{b}_{k+1} - \bar{\mathbf{b}}_{k+1}) \end{aligned} \quad (30)$$

with  $\delta \mathbf{b}_{k+1} = \mathbf{b}_{k+1} - \bar{\mathbf{b}}_{k+1}$  for convenience. Inserting the expanded dynamics (27), (28) into the second term of (25), i.e. (30), and evaluating the expectation over  $\xi_k$  yields

$$\mathbb{E}_{\xi_k} [V_{k+1}^i(g_k(\mathbf{s}_k) + W_k(\mathbf{s}_k)\xi_k)] \quad (31)$$

$$\begin{aligned} &\approx \mathbb{E}_{\xi_k} \left[ V_{k+1}^i + V_{\mathbf{b},k+1}^{i,\top} (g_k(\mathbf{s}_k) + W_k(\mathbf{s}_k)\xi_k - \bar{\mathbf{b}}_{k+1}) \right. \\ &\quad \left. + \frac{1}{2} (g_k(\mathbf{s}_k) + W_k(\mathbf{s}_k)\xi_k - \bar{\mathbf{b}}_{k+1})^\top V_{\mathbf{bb},k+1}^i (g_k(\mathbf{s}_k) + \right. \\ &\quad \left. W_k(\mathbf{s}_k)\xi_k - \bar{\mathbf{b}}_{k+1}) \right] \quad (32) \end{aligned}$$

$$= V_{k+1}^i + V_{\mathbf{b},k+1}^{i,\top} (g_k(\mathbf{s}_k) - \bar{\mathbf{b}}_{k+1}) \quad (33)$$

$$+ \frac{1}{2} (g_k(\mathbf{s}_k) - \bar{\mathbf{b}}_{k+1})^\top V_{\mathbf{bb},k+1}^i (g_k(\mathbf{s}_k) - \bar{\mathbf{b}}_{k+1})$$

$$+ \frac{1}{2} \text{tr} (W_k(\mathbf{s}_k)^\top V_{\mathbf{bb},k+1}^i W_k(\mathbf{s}_k))$$

$$= V_{k+1}^i + V_{\mathbf{b},k+1}^{i,\top} g_{\mathbf{s},k} \delta \mathbf{s}_k + \frac{1}{2} \delta \mathbf{s}_k^\top g_{\mathbf{s},k}^\top V_{\mathbf{bb},k+1}^i g_{\mathbf{s},k} \delta \mathbf{s}_k \quad (34)$$

$$+ \frac{1}{2} \sum_{j=1}^{n_x} (W_k^{(j)} + W_{\mathbf{s},k}^{(j)} \delta \mathbf{s}_k)^\top V_{\mathbf{bb},k+1}^i (W_k^{(j)} + W_{\mathbf{s},k}^{(j)} \delta \mathbf{s}_k)^\top.$$

Here we use the value function expansion (30) in (32), and the fact that  $\bar{\mathbf{b}}_{k+1} = g_k(\bar{\mathbf{s}}_k)$  in (33) in the form of

$$g_k(\mathbf{s}_k) - \bar{\mathbf{b}}_{k+1} = g_k(\mathbf{s}_k) - g_k(\bar{\mathbf{s}}_k) = g_{\mathbf{s},k} \delta \mathbf{s}_k. \quad (35)$$

Collecting and grouping all first and second order terms of (34) and (26) we have that the resulting  $Q_k^i(\bar{\mathbf{s}}_k + \delta \mathbf{s}_k)$  is a quadratic with coefficients given by (22 - 24). ■

For notational convenience we will drop the time index  $k$  for the  $Q$  matrices. We can also recover other partial derivatives of  $Q^i$  from (22 - 24):

$$Q_{\mathbf{s}}^i = \begin{bmatrix} Q_{\mathbf{b}}^i \\ Q_{\mathbf{u}^1}^i \\ \vdots \\ Q_{\mathbf{u}^N}^i \end{bmatrix}, \quad Q_{\mathbf{ss}}^i = \begin{bmatrix} Q_{\mathbf{bb}}^i & Q_{\mathbf{bu}^1}^i & \cdots & Q_{\mathbf{bu}^N}^i \\ Q_{\mathbf{u}^1 \mathbf{b}}^i & Q_{\mathbf{u}^1 \mathbf{u}^1}^i & \cdots & Q_{\mathbf{u}^1 \mathbf{u}^N}^i \\ \vdots & \vdots & \ddots & \vdots \\ Q_{\mathbf{u}^N \mathbf{b}}^i & Q_{\mathbf{u}^N \mathbf{u}^1}^i & \cdots & Q_{\mathbf{u}^N \mathbf{u}^N}^i \end{bmatrix}. \quad (36)$$

With  $Q_k^i(\bar{\mathbf{s}}_k + \delta \mathbf{s}_k)$  in quadratic form from Theorem 2, at stage  $k$  each agent  $i$  solves the quadratic problem

$$\delta \mathbf{u}_k^{i,*} = \arg \min_{\delta \mathbf{u}_k^i} Q_{\mathbf{s},k}^{i,\top} \delta \mathbf{s}_k + \frac{1}{2} \delta \mathbf{s}_k^\top Q_{\mathbf{ss},k}^i \delta \mathbf{s}_k, \quad (37)$$

yielding a quadratic game in the variables  $\mathbf{u}_k$  with a unique and simple to compute solution [28]. Theorem 3 presents this solution.

**Theorem 3.** *The solution to the quadratic game (37) is given by*

$$\delta \mathbf{u}_k^* = -\hat{Q}_{\mathbf{u}\mathbf{u}}^{-1} \left( \hat{Q}_{\mathbf{u}} + \hat{Q}_{\mathbf{u}\mathbf{b}} \delta \mathbf{b}_k \right) \quad (38)$$

where  $\hat{Q}_{\mathbf{u}\mathbf{u}}$ ,  $\hat{Q}_{\mathbf{u}\mathbf{b}}$ ,  $\hat{Q}_{\mathbf{u}}$ , are populated from (36), and defined

$$\hat{Q}_{\mathbf{u}\mathbf{u}} = \begin{bmatrix} Q_{\mathbf{u}^1\mathbf{u}}^1 \\ Q_{\mathbf{u}^2\mathbf{u}}^2 \\ \vdots \\ Q_{\mathbf{u}^N\mathbf{u}}^N \end{bmatrix}, \quad \hat{Q}_{\mathbf{u}\mathbf{b}} = \begin{bmatrix} Q_{\mathbf{u}^1\mathbf{b}}^1 \\ Q_{\mathbf{u}^2\mathbf{b}}^2 \\ \vdots \\ Q_{\mathbf{u}^N\mathbf{b}}^N \end{bmatrix}, \quad \hat{Q}_{\mathbf{u}} = \begin{bmatrix} Q_{\mathbf{u}^1}^1 \\ Q_{\mathbf{u}^2}^2 \\ \vdots \\ Q_{\mathbf{u}^N}^N \end{bmatrix}. \quad (39)$$

*Proof:* By taking the derivative of the objective of (37) and equating it to zero, the stationarity condition of (37) yields

$$\begin{bmatrix} Q_{\mathbf{u}^i\mathbf{u}^i}^i & Q_{\mathbf{u}^i\mathbf{u}^{-i}}^i \end{bmatrix} \begin{bmatrix} \delta \mathbf{u}_k^i \\ \delta \mathbf{u}_k^{-i} \end{bmatrix} + Q_{\mathbf{u}^i\mathbf{b}}^i \delta \mathbf{b}_k + Q_{\mathbf{u}^i}^i = 0. \quad (40)$$

Stacking the stationarity conditions of all  $N$  agents into a single system of equations we find

$$\hat{Q}_{\mathbf{u}\mathbf{u}} \delta \mathbf{u}_k + \hat{Q}_{\mathbf{u}\mathbf{b}} \delta \mathbf{b}_k + \hat{Q}_{\mathbf{u}} = 0, \quad (41)$$

where (38) is the solution to this system of equations. ■

The local necessary condition of Problem 2, derived in Section III-B holds.

**Corollary 1.** *The solution (38) fulfills the necessary condition of the local Nash equilibrium (19) at time  $k$ .*

*Proof:* From (40), we see  $\frac{\partial Q_k^i(\mathbf{b}_k, \mathbf{u}_k)}{\partial \mathbf{u}_k^i} = 0$ . ■

We can immediately derive the linear feedback policy for all agents at planning time  $k$  of the form

$$\pi_k = \bar{\mathbf{u}}_k + j_k + K_k \delta \mathbf{b}_k \quad (42)$$

with  $j_k = -\hat{Q}_{\mathbf{u}\mathbf{u}}^{-1} \hat{Q}_{\mathbf{u}}$  the feed forward term and  $K_k = -\hat{Q}_{\mathbf{u}\mathbf{u}}^{-1} \hat{Q}_{\mathbf{u}\mathbf{b}}$  the feedback term. Note that  $\pi_k$  contains the optimal policy of the robot  $\pi_k^0$  and also the predicted policies for all other (N-1) agents  $\pi_k^{-0}$ . The interdependence has been resolved by solving (41).

We now formulate the backwards equations to propagate the value functions  $V^i$  backwards, hence defining the backward pass.

**Corollary 2.** *The discrete backwards differential equations of the value functions  $V^i$  are*

$$V_k^i = Q^i + Q_{\mathbf{u}^i}^{i\top} j_k + \frac{1}{2} j_k^\top Q_{\mathbf{u}\mathbf{u}}^i j_k \quad (43)$$

$$V_{\mathbf{b},k}^i = Q_{\mathbf{b}}^i + K_k^\top Q_{\mathbf{u}\mathbf{u}}^i j_k + K_k^\top Q_{\mathbf{u}}^i + Q_{\mathbf{u}\mathbf{b}}^{i\top} j_k \quad (44)$$

$$V_{\mathbf{b}\mathbf{b},k}^i = Q_{\mathbf{b}\mathbf{b}}^i + K_k^\top Q_{\mathbf{u}\mathbf{u}}^i K_k + K_k^\top Q_{\mathbf{u}\mathbf{b}}^i + Q_{\mathbf{u}\mathbf{b}}^{i\top} K_k, \quad (45)$$

with terminal constraints

$$V_l^i = \partial c_l^i(\bar{\mathbf{b}}_l), \quad V_{\mathbf{b},l}^i = \left. \frac{\partial c_l^i(\mathbf{b})}{\partial \mathbf{b}} \right|_{\mathbf{b}=\bar{\mathbf{b}}_l}, \quad V_{\mathbf{b}\mathbf{b},l}^i = \left. \frac{\partial^2 c_l^i(\mathbf{b})}{\partial \mathbf{b}^2} \right|_{\mathbf{b}=\bar{\mathbf{b}}_l}. \quad (46)$$

*Proof:* Substituting the solution (38) and (42) back into the quadratic (21) yields the value function  $V_k^i(\bar{\mathbf{b}}_k + \delta \mathbf{b}_k)$ .

$$\begin{aligned} V_k^i(\bar{\mathbf{b}}_k + \delta \mathbf{b}_k) &= Q_k^i(\bar{\mathbf{b}}_k + \delta \mathbf{b}_k, \pi_k) \\ &= Q^i + Q_{\mathbf{u}^i}^{i\top} (j_k + K_k \delta \mathbf{b}_k) + Q_{\mathbf{b}}^{i\top} \delta \mathbf{b}_k \\ &\quad + \frac{1}{2} (j_k + K_k \delta \mathbf{b}_k)^\top Q_{\mathbf{u}\mathbf{u}}^i (j_k + K_k \delta \mathbf{b}_k) + \frac{1}{2} \delta \mathbf{b}_k^\top Q_{\mathbf{b}\mathbf{b}}^i \delta \mathbf{b}_k \\ &\quad + \frac{1}{2} (j_k + K_k \delta \mathbf{b}_k)^\top Q_{\mathbf{u}\mathbf{b}}^i \delta \mathbf{b}_k + \frac{1}{2} \delta \mathbf{b}_k^\top Q_{\mathbf{b}\mathbf{u}}^i (j_k + K_k \delta \mathbf{b}_k) \end{aligned}$$

Collecting first and second order terms in  $\delta \mathbf{b}_k$  gives the Equations (43-45) in the form of (30). The terminal constraints (46) result from a Taylor expansion of the final cost  $c_l^i$  around the final nominal belief  $\bar{\mathbf{b}}_l$ . ■

Based on results of Theorem 3 and Corollary 2 we can propagate the quadratic value functions backwards in time starting from the terminal constraints at time  $l$ .

### D. Regularization

With any Newton-like method, care must be taken when the Hessian  $\hat{Q}_{\mathbf{u}\mathbf{u}}$  is not positive-definite or when the minimum is not close and the quadratic model inaccurate. To ensure that the algorithm converges regardless of initial conditions, we implement a Levenberg-Marquardt style regularization [32].

1) *Control Regularization:* The control regularization is achieved by adding a diagonal term of magnitude  $\mu_{\mathbf{u}}$  to the diagonal of  $\hat{Q}_{\mathbf{u}\mathbf{u}}$ , yielding

$$\tilde{Q}_{\mathbf{u}\mathbf{u}}^i = \hat{Q}_{\mathbf{u}\mathbf{u}}^i + \mu_{\mathbf{u}} I. \quad (47)$$

This simple Levenberg-Marquardt style modification results in adding a quadratic cost around the current control sequence, which forces the new optimal control inputs computed by the backward pass to stay closer to the previous iteration.

2) *Belief Regularization:* The drawback of the control based regularization scheme is that even small control perturbations can cause large deviations in the state trajectory potentially inhibiting convergence. To ensure that the updated belief trajectory does not deviate too far from the previous iteration, we introduce a scheme that penalizes deviations from beliefs rather than controls with parameter  $\mu_{\mathbf{b}}$ :

$$\begin{aligned} \tilde{Q}_{\mathbf{ss},k}^i &= c_{\mathbf{ss},k}^i + g_{\mathbf{s},k}^\top (V_{\mathbf{b}\mathbf{b},k+1}^i + \mu_{\mathbf{b}} I) g_{\mathbf{s},k} \\ &\quad + \sum_{i=1}^n W_{\mathbf{s},k}^{(j),T} (V_{\mathbf{b}\mathbf{b},k+1}^i + \mu_{\mathbf{b}} I) W_{\mathbf{s},k}^{(j)}. \end{aligned} \quad (48)$$

The outcome of the state based regularization is placing a quadratic belief-cost around the previous belief trajectory, similar to [33] where a state based regularization was employed. In contrast to the standard control-based regularization, the feedback gains  $K_k$  do not go to zero as  $\mu_{\mathbf{b}} \rightarrow \infty$ , but rather force the new trajectory closer to the old one. In practice, we find this improves the robustness of convergence.

### E. Algorithm for Dynamic Game Belief Space Planning

We summarize our findings in Algorithm 1, solving for Nash equilibria of dynamic games in belief space. Theorem 2 lays the foundation for the quadratic game solved in the

backward pass of Algorithm 1. The solution to the quadratic game presented in Theorem 3 yields a linear feedback policy  $\pi_k$  for all agents. We propagate the value function in the backwards pass according to Corollary 2 starting with the terminal conditions from the terminal cost. We update the nominal control and belief trajectories in the forward pass based on rolling out the belief dynamics model and applying the updated feedback policy  $\pi_k$ . If all agents' action-value functions improved, we accept the updated nominal belief and control trajectories and reduce regularization. Otherwise the trajectories are rejected and the regularization is increased. The iteration of backward and forward pass continues until each agents' action value function  $Q^i$  converges and changes less than a specified threshold  $\epsilon$ .

---

**Algorithm 1** Nash Equ. of Dynamic Games in Belief Space
 

---

**Input:** Initial trajectories  $\bar{\mathbf{b}}, \bar{\mathbf{u}}$ , functions  $c_k^i, c_l^i, f, h$

**Output:** Predicted trajectories  $\bar{\mathbf{b}}, \bar{\mathbf{u}}$ , feedback law  $\pi$

```

1: while  $|Q^i(\bar{\mathbf{b}}_{\text{new}}, \bar{\mathbf{u}}_{\text{new}}) - Q^i(\bar{\mathbf{b}}, \bar{\mathbf{u}})| > \epsilon$  do
2:   Backward pass:
3:    $V_{\mathbf{b},l}^i, V_{\mathbf{bb},l}^i \leftarrow$  From terminal boundary conditions (46)
4:   for  $k$  from  $l-1$  to  $0$  do
5:      $\pi_k^i, j_k^i, K_k^i \leftarrow$  Solve quadratic game (42)
6:      $V_{\mathbf{b},k}^i, V_{\mathbf{bb},k}^i \leftarrow$  Propagate value function (44, 45)
7:   end for
8:   Forward pass:
9:    $\bar{\mathbf{b}}_{\text{new}}, \bar{\mathbf{u}}_{\text{new}} \leftarrow$  Propagate  $\mathbf{b}_0$  with  $g$  and  $\pi$ 
10:  if  $Q^i(\bar{\mathbf{b}}_{\text{new}}, \bar{\mathbf{u}}_{\text{new}}) \leq Q^i(\bar{\mathbf{b}}, \bar{\mathbf{u}})$  then
11:     $\bar{\mathbf{b}}, \bar{\mathbf{u}} \leftarrow \bar{\mathbf{b}}_{\text{new}}, \bar{\mathbf{u}}_{\text{new}}$ ,
12:    lower regularization (47, 48)
13:  else increase regularization
14:  end if
15: end while

```

---

The algorithm yields a linear feedback policy  $\pi^0$  of robot 0 over the time full time horizon, as well as predicted feedback policies  $\pi^{-0}$  and predicted belief trajectories  $\mathbf{b}^{-0}$  for all other agents.

Per iteration of Algorithm 1  $l$  quadratic games are solved such that its runtime scales linearly  $\mathcal{O}(l)$  in the planning horizon  $l$ . We benefit from improved scaling during real-time deployment whereas other POMDP algorithms, even without taking any game dynamics into account, scale exponentially.

#### IV. CASE STUDIES

We demonstrate the performance and flexibility of our Algorithm 1 using three case studies that combine the information-seeking behavior with our game theoretic formulation. These case studies examine how the agents: play the game, gain information, and use the information gain to improve their control policies. We choose these illustrative examples due to their variations in agent interactions and demonstration of broader capabilities. Each of the case studies employs a different dynamics and observation model as well as distinct objectives for the agents. We find the Nash equilibrium to each of these games using Algorithm 1.

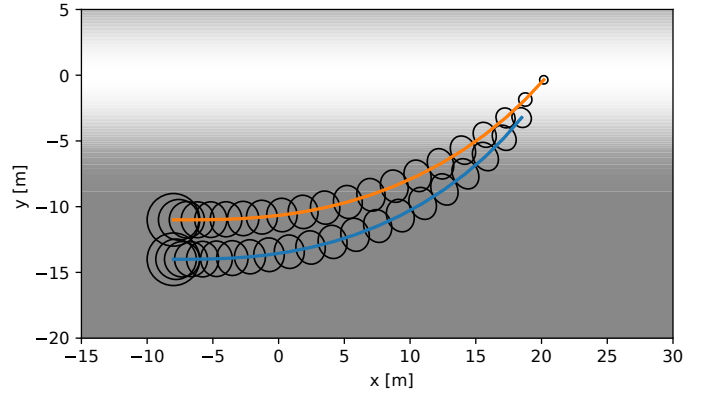


Fig. 2. Agent 1 (blue) is pushing Agent 2 (orange) into the light to reduce the uncertainty over Agent 2 at the end of the planning horizon. Uncertainties are visualized by covariance ellipses.

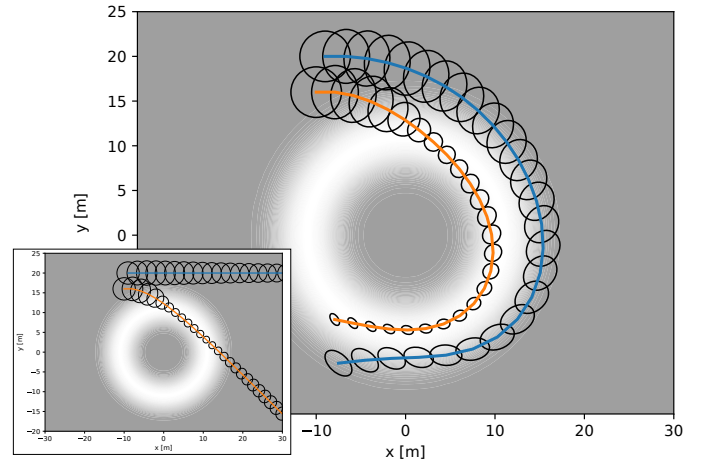


Fig. 3. By nudging Agent 2 onto the circular light source Agent 1 is able to reduce the uncertainty over Agent 1's state at the end of the planning horizon. The lower left inset shows the same scenario without any information gain. As a result, Agent 1 has no incentive to manipulate Agent 2's behavior since there is no way to influence its uncertainty.

##### A. Active Surveillance

In this case study, Agents 1 and 2 are in an environment with variable lighting conditions. Agent 1 is tasked with observing Agent 2, but the quality of the observations depends on the available lighting at that point of the environment. Agent 2 has no goal, but is assigned the objective of maintaining a constant velocity while avoiding Agent 1. Neither agent has perfect information of the other, only a noisy position estimate forming the initial belief. Using our approach, we show that Agent 1 can successfully herd Agent 2 into the lighted region to achieve its surveillance objective, which would not be possible without incorporating the belief space planning into the dynamic game. Figures 2 and 3 show the trajectories in two environments.

The state of both car-like robots  $\mathbf{x}^{(i)} = [x^{(i)}, y^{(i)}, \theta^{(i)}, v^{(i)}]$  consists of their position  $(x, y)$ , orientation  $\theta$ , and speed  $v$ . The control inputs  $\mathbf{u}^{(i)} = [u_{\text{acc},k}^{(i)}, u_{\text{steer},k}^{(i)}]$  are acceleration  $u_{\text{acc},k}$  and steering wheel angle  $u_{\text{steer},k}$ . The deterministic continuous



dynamics of both agents are given by

$$\dot{\mathbf{x}}_k^{(i)} = \left[ v_k^{(i)} \cos \theta_k^{(i)}, v_k^{(i)} \sin \theta_k^{(i)}, u_{\text{acc},k}^{(i)}, \frac{v_k^{(i)}}{L \tan(u_{\text{steer},k}^{(i)})} \right]^\top,$$

where  $L$  is the length of the robots. The discrete time dynamics are defined by

$$\mathbf{x}_k = f(\mathbf{x}_k, \mathbf{u}_k, \mathbf{m}_k) = \mathbf{x}_k + \dot{\mathbf{x}}_k \tau + M(\mathbf{u}_k) \cdot \mathbf{m}_k,$$

for timestep  $\tau$  and  $M(\mathbf{u}_k)$  scales the motion noise  $\mathbf{m}_k$  proportional to the control input  $\mathbf{u}_k$ , such that uncertainty increases if excessive controls are executed. We encode the agents objective and goals in this game by defining the current and terminal costs for Agent 1 and Agent 2 as

$$\begin{aligned} c_k^{(1)}(\mathbf{b}_k, \mathbf{u}_k) &= \mathbf{u}_k^{(1)\top} R \mathbf{u}_k^{(1)}, \\ c_l^{(1)}(\mathbf{b}_l) &= \det(\Sigma_{x,y}^{(2)}), \\ c_k^{(2)}(\mathbf{b}_k, \mathbf{u}_k) &= \mathbf{u}_k^{(2)\top} R \mathbf{u}_k^{(2)} + a_1(v_k^{(2)} - v_{k,\text{des}}^{(2)})^2 + a_2 c_{\text{coll}}(\mathbf{x}_k), \\ c_l^{(2)}(\mathbf{b}_l) &= a_1(v_l^{(2)} - v_{l,\text{des}}^{(2)})^2 + a_2 c_{\text{coll}}(\mathbf{x}_l). \end{aligned}$$

Agent 1’s overall objective is to lower the uncertainty about the position of Agent 2 at the end of the planning horizon, encoded by  $c_l^{(1)}(\mathbf{b}_l)$ . The term  $\det(\Sigma_{x,y}^{(2)})$  is equivalent to the area of the  $1\sigma$ -threshold ellipse of Agent 2 and representative of the location uncertainty of Agent 2 at the end of the planning horizon. Note that both agents penalize control effort by  $\mathbf{u}_k^{(i)\top} R \mathbf{u}_k^{(i)}$ , and Agent 2 has additional objectives for maintaining a desired velocity  $v_{\text{des}}$  and avoiding collisions via an exponential barrier  $c_{\text{coll}}(\mathbf{x}_k) = \exp(-d(\mathbf{x}_k))$ , where  $d(\mathbf{x}_k)$  is the expected euclidean distance until collision between the two agents, taking their outline into account.

We restrict the robots’ sensing abilities to only include noisy position measurements. The observation model varies across the environment based on the available light at a particular location,

$$\mathbf{z}_k^{(i)} = h(\mathbf{x}_k^{(i)}, \mathbf{n}_k^{(i)}) = [x_k^{(i)}, y_k^{(i)}]^T + N(\mathbf{x}_k^{(i)}) \cdot \mathbf{n}_k^{(i)},$$

where the matrix  $N(\mathbf{x}_k^{(i)})$  scales the measurement noise based on the current position  $(x, y)$  in the map. We show the nominal trajectories and the associated beliefs of the solution computed using Algorithm 1 in Figures 2 and 3. In both cases Agent 1 (blue) is able to force Agent 2 into the light to successfully reduce uncertainty. The emergent behavior would not have been possible without belief-space planning, reasoning about another agent’s uncertainty, and without the dynamic game, estimating how the own actions influence another agent’s actions. We show the resulting behavior without belief space planning and without any reasoning about Agent 2’s uncertainty in the inset of Figure 3.

### B. Guide Dog for Blind Agent

In this scenario, Agent 2 guides Agent 1 towards a goal location while choosing a path that reduces the uncertainty in Agent 1’s position. The game is won if Agent 1 knows it reaches the goal location with a low uncertainty about its state, however, Agent 1 does not have the ability to navigate

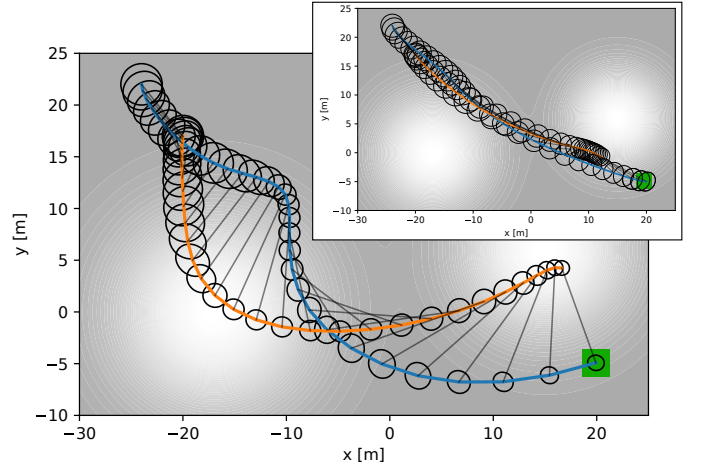


Fig. 4. Guide dog (orange) with leash (black line) guides the blind agent (blue) towards the goal location (green). While doing so it passes by both light sources to reduce the uncertainty of the blind person’s position at the goal location. The top right inset shows the case where the guide dog is indifferent about the blind person’s uncertainty.

itself. We refer to Agent 1 as the “blind” agent. Following this analogy, Agent 2 acts as the “guide dog” for the blind agent. The guide dog can gather information about its own state and the blind agent’s state by passing through light sources in the environment which reduces uncertainty. The agents are tethered together, which we model with spring dynamics and refer to the tether as the “leash.” If the guide takes the blind agent on the direct path to the goal, the guide would not have sufficient information to know it brought the blind agent to the goal location. Under our approach, the guide dog detours to key areas to reduce the blind agent’s uncertainty. We use the analogy of a guide dog leading a blind agent to create an intuitive visual for the reader, however, this system is relevant to many other robotic applications.

We model the system dynamics as two masses on a surface with friction connected by a spring tether. The states of blind agent and guide dog are  $\mathbf{x}^{(i)} = [\mathbf{r}^{(i)}, \mathbf{v}^{(i)}]$  the 2D position  $\mathbf{r}$  and velocities  $\mathbf{v}$ . The inputs  $\mathbf{u}^{(i)} = F^{(i)}$  are their respective force vectors. The blind agent and guide dog have masses  $c_{\text{mass},h}$  and  $c_{\text{mass},d}$  respectively and are bound to friction coefficients  $c_{\text{fric},h}$  and  $c_{\text{fric},d}$ . The accelerations are

$$\begin{aligned} \mathbf{a}^{(1)} &= 1/c_{\text{mass},h}(\mathbf{u}^{(1)} - f_{\text{spring}}(\Delta\mathbf{r}) - c_{\text{fric},h}\mathbf{v}^{(1)}), \\ \mathbf{a}^{(2)} &= 1/c_{\text{mass},d}(\mathbf{u}^{(2)} + f_{\text{spring}}(\Delta\mathbf{r}) - c_{\text{fric},d}\mathbf{v}^{(2)}), \end{aligned}$$

and influenced by the spring force

$$f_{\text{spring}}(\Delta\mathbf{r}) = \frac{\Delta\mathbf{r}}{\|\Delta\mathbf{r}\|} c_{\text{spring}} \max(\|\Delta\mathbf{r}\| - c_{\text{leash}}, 0),$$

which is dependent on the distance vector  $\Delta(\mathbf{r}) = [\mathbf{r}^{(1)} - \mathbf{r}^{(2)}]$ . The dog’s leash is flexible with spring constant  $c_{\text{spring}}$  and has length  $c_{\text{leash}}$ , such that it only generates a spring force if extended beyond  $c_{\text{leash}}$  and is otherwise slack. The deterministic continuous dynamics are  $\dot{\mathbf{x}}^{(i)} = [\mathbf{v}^{(i)\top}, \mathbf{a}^{(i)\top}]^\top$ , and the discrete time dynamics

$$f(\mathbf{x}_k, \mathbf{u}_k, \mathbf{m}_k) = \mathbf{x}_k + \dot{\mathbf{x}}_k \tau + M(\mathbf{u}_k) \cdot \mathbf{m}_k,$$

for timestep  $\tau$  and where  $M(\mathbf{u}_k)$  scales the motion noise proportional to the inputs  $\mathbf{u}_k$ .

We use the cost functions to encode the behaviors and objects of each agent. Similar to the previous case study, minimizing  $\det(\Sigma_{r,l}^{(1)})$  reduces the uncertainty at the end of the planning horizon. We define

$$\begin{aligned} c_k^{(1)}(\mathbf{b}_k, \mathbf{u}_k) &= \mathbf{u}_k^{(1),\top} R \mathbf{u}_k^{(1)} + c_{\text{acc,h}} \mathbf{a}_k^{(1),\top} \mathbf{a}_k^{(1)}, \\ c_l^{(1)}(\mathbf{b}_l) &= 0, \\ c_k^{(2)}(\mathbf{b}_k, \mathbf{u}_k) &= \mathbf{u}_k^{(2),\top} R \mathbf{u}_k^{(2)}, \\ c_l^{(2)}(\mathbf{b}_l) &= \det(\Sigma_{r,l}^{(1)}) + \|\mathbf{r}_l^{(1)} - \mathbf{r}_{\text{goal}}\|^2. \end{aligned}$$

Here, the term  $\|\mathbf{r}_l^{(1)} - \mathbf{r}_{\text{goal}}\|^2$  drives the guide dog to relocate the blind agent to the goal. We reduce the control efforts of each agent by  $\mathbf{u}_k^{(i),\top} R \mathbf{u}_k^{(i)}$ , and the blind agent has the additional objective of reducing accelerations with  $c_{\text{acc,h}} \mathbf{a}_k^{(1),\top} \mathbf{a}_k^{(1)}$ . We use a noisy observation model

$$\mathbf{z}_k^{(i)} = h(\mathbf{x}_k^{(i)}, \mathbf{n}_k^{(i)}) = \mathbf{x}_k^{(i)} + N(\mathbf{x}_k^{(i)}) \cdot \mathbf{n}_k^{(i)}, \quad (49)$$

where the matrix  $N(\mathbf{x}_k^{(i)})$  scales the measurement noise based on the environment shown in Figure 4.

The resulting behavior is shown in Figure 4: The dog (orange) guides the blind agent (blue) from its initial position to the blind person's goal location (green) while reducing the uncertainty of the blind agent's final state by planning a slight detour through the light sources instead of directly towards the goal location. The guide does so while also taking the complex interaction originating from the blind person's forces on the tether into account. The inset on Figure 4 is the path taken by the dog with no optimization over the blind agent's uncertainty. While it takes a direct path to the goal, the final uncertainty of the blind agent is large.

### C. Autonomous Racing

Finally, we demonstrate our approach in competitive racing, a common problem in dynamic games. By incorporating belief space planning into the dynamic game formulation, we show a significant increase in racing performance. This allows the agents to reduce uncertainty and decrease chance constraints, thus maneuvers like overtaking on tight road segments become possible.

In all racing runs each agent maintains a separate instance of Algorithm 1. This means that each agent separately computes their own optimal control actions, the predictions of other respective agents, and each agent computes their own Nash equilibrium. Additionally, no information is shared among agents. Since each agent runs a separate instance of Algorithm 1, Assumption 1 ( $\mathbf{b}^{ij} \approx \mathbf{b}^{ii}$ ) may or may not be accurate, i.e. the belief computed by agent  $j$  over agent  $i$  may only inaccurately resemble the belief of agent  $i$  over itself. Nonetheless, we will show that despite a first-order belief assumption, the presented approach yields superior performance to all other baselines.

Each agent's state  $\mathbf{x}^{(i)} = [x^{(i)}, y^{(i)}, \theta^{(i)}, v^{(i)}]$  and controls  $\mathbf{u}^{(i)} = [u_{\text{acc},k}^{(i)}, u_{\text{steer},k}^{(i)}]$  are the same as in the active surveillance

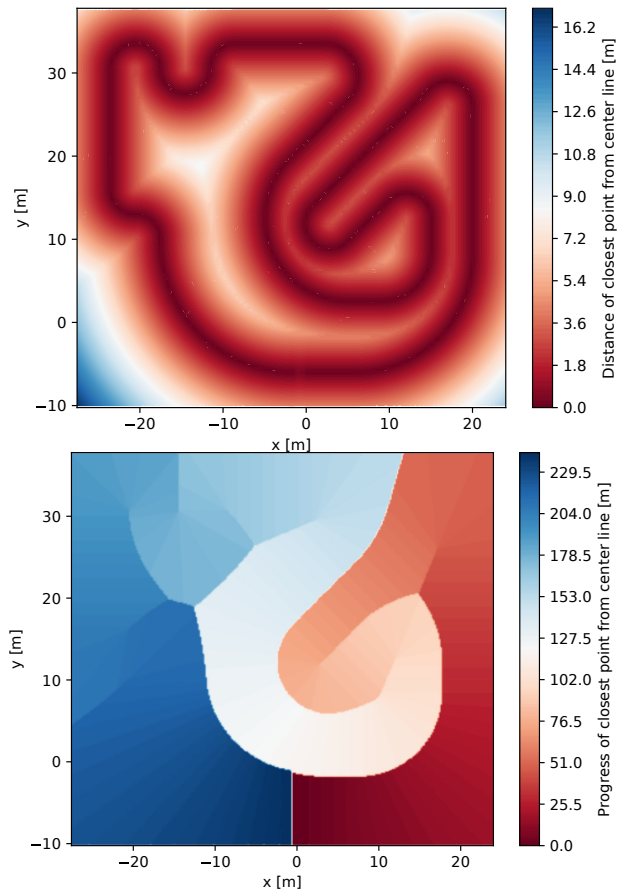


Fig. 5. **Top: (Distance Transform)** Map of the distances to the closest point on the center line  $d(\mathbf{p})$  of the race track shown in Figure 1. **Bottom: (Progress Transform)** Map of the progress  $r(\mathbf{p})$  along the race track of the closest point on the center line.

experiment but the different deterministic continuous dynamics are of the form

$$\begin{aligned} \dot{\mathbf{x}}_k^{(i)} &= [v_k^{(i)} \cos(\theta_k^{(i)}), v_k^{(i)} \sin(\theta_k^{(i)}), \\ &\quad u_{\text{acc},k}^{(i)} - c_{\text{drag},i} v_k^{(i)} - c_{\text{slip},i} (\dot{\theta}^{(i)})^2, \dot{\theta}^{(i)}]^\top, \end{aligned}$$

with yaw rate  $\dot{\theta}^{(i)} = v_k^{(i)} / L \tan(u_{\text{steer},k}^{(i)})$ , and drag-  $c_{\text{drag},i}$  and slip coefficient  $c_{\text{slip},i}$ . The stochastic discrete time dynamics,

$$\mathbf{x}_k = f(\mathbf{x}_k, \mathbf{u}_k, \mathbf{m}_k) = \mathbf{x}_k + \dot{\mathbf{x}}_k \tau + M(\mathbf{b}_k, \mathbf{u}_k) \cdot \mathbf{m}_k,$$

are subject to noise scaled by  $M(\mathbf{b}_k, \mathbf{u}_k)$  proportional to the control input  $\mathbf{u}_k$  as well as the squared yaw rate  $(\dot{\theta}^{(i)})^2$  of each agent  $i$  separately. The observation model

$$\mathbf{z}_k^{(i)} = h(\mathbf{x}_k^{(i)}, \mathbf{n}_k^{(i)}) = \mathbf{x}_k^{(i)} + N(\mathbf{x}_k^{(i)}) \cdot \mathbf{n}_k^{(i)},$$

is subject to noise scaled by  $N(\mathbf{x}_k^{(i)})$ , depending on the position on the race track map. As shown in Figure 1, we indicate zones of low measurement noise as red. It may be beneficial for agents to plan to drive through these low measurement noise regions to increase information gain and to reduce uncertainty.

Each agent's goal is to maximize progress along the race track while staying on the track and not colliding with other

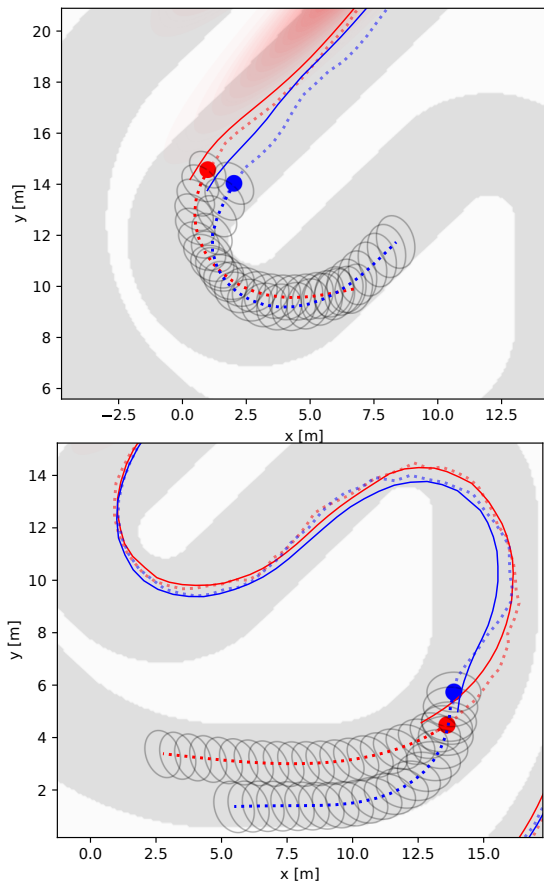


Fig. 6. **Top:** Blue agent cuts in front of the red agent, forcing the red agent to break. As a result, the blue agent can remain in front of the red agent at the end of the turn. **Bottom:** The red agent blocks the blue agent’s overtaking maneuver forcing the blue agent to stay behind and take a wider line in the upcoming right turn. Significant amount of noise is simulated visualized by the deviation of the true trajectory (solid lines) and the predicted mean of the belief (dashed lines).

agents. We define the progress along the track for any point  $\mathbf{p} = (x, y)$  as arc-length progress  $r(\mathbf{p})$  of the closest point on the centerline. Likewise, we define  $d(\mathbf{p})$  as the distance of the closest point on the track to  $\mathbf{p}$ . We visualize both the distance transform as well as the progress transform of the race track shown from Figure 1 in Figure 5. For competitive racing, each agent tries to maximize the relative progress over other agents  $r(\mathbf{p}^{(i)}) - r(\mathbf{p}^{(-i)})$ . Consequently, agents will engage in competitive blocking and cutting behavior. We design the current and terminal costs of each agent as

$$\begin{aligned} c_k^{(i)}(\mathbf{b}_k, \mathbf{u}_k) &= \mathbf{u}_k^{(i),\top} R \mathbf{u}_k^{(i)} + c_{\text{track}}^{(i)}(\mathbf{b}_k) + c_{\text{coll}}^{(i)}(\mathbf{b}_k), \\ c_l^{(i)}(\mathbf{b}_l) &= -r(p_l^{(i)}) + r(p_l^{(-i)}), \end{aligned}$$

penalizing control effort by  $R$ , while  $c_{\text{track}}^{(i)}(\mathbf{b}_k)$  and  $c_{\text{coll}}^{(i)}(\mathbf{b}_k)$  keep the agent on the track and out of collision. We achieve this by finding the upper bound of the  $2\sigma$  positional uncertainty  $\Sigma_{x,y}^{(i)}$  as  $\alpha = 2\sqrt{\max(\text{eig}(\Sigma_{x,y}^{(i)}))}$ . We can then formulate a chance collision constraint with other agents (limiting  $\|\mathbf{p}^{(i)} - \mathbf{p}^{(j)}\|$ ) and the boundary of the race track (limiting  $d(\mathbf{p})$ ) by restricting positions in the  $\alpha$  vicinity. Finally, to arrive at  $c_{\text{track}}^{(i)}(\mathbf{b}_k)$  and  $c_{\text{coll}}^{(i)}(\mathbf{b}_k)$  we convert the constraints to

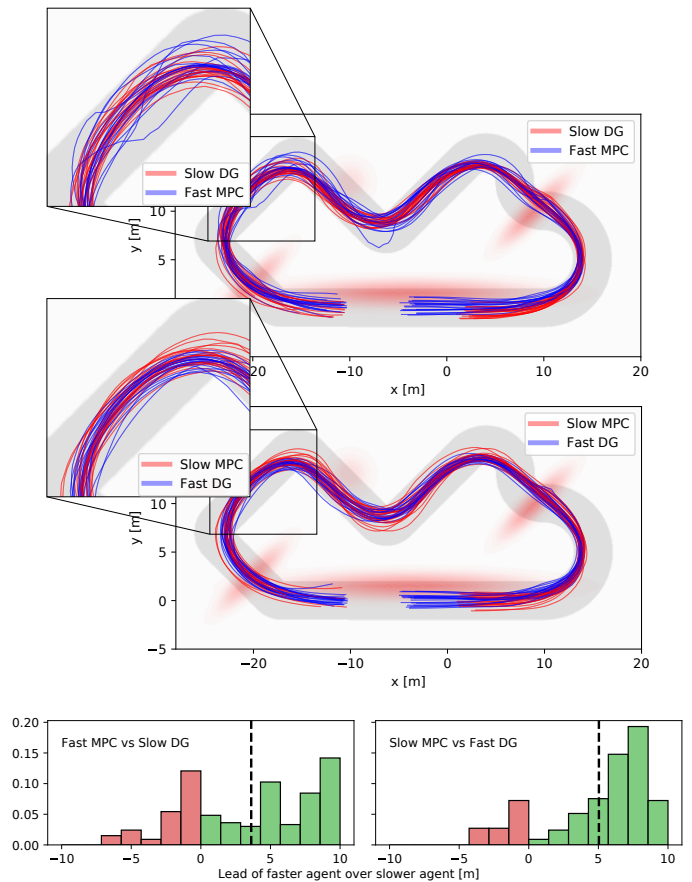


Fig. 7. **Top:** Traces of agents comparing MPC and DG. In both cases the MPC method moves away from the ideal racing line more often due to failed overtaking attempts. It can not foresee its influence on the DG agent’s actions and thus is less efficient. It is also not able to take advantage of estimating its implicit control over the other agent like the DG agent. **Bottom:** Histograms of the  $\Delta$ arc-length lead of the faster agent over the slower agent. Green indicates that the faster agent won the race against the agent starting in the lead, whereas red indicates the opposite. In comparison, the DG method won more races than the MPC method and had a higher average lead.

soft constraints, penalizing constraint violation exponentially strong, as suggested in [29]. Additionally, we also limit control inputs  $\mathbf{u}_k$  by soft constraints.

1) *Competitive Racing:* In our racing simulation, each car executes the current commanded control computed by their own separate instance of Algorithm 1, and the dynamics subject to noise are propagated forward. Subsequently, a noisy observation is generated and the current belief is updated by an EKF step. Each agent runs an individual EKF, maintains their own separate belief over themselves and others, and receives noisy measurements with independently generated noise for each agent. No information is shared apart from cost and dynamics models. To test robustness we simulate substantial amounts of noise, such that the belief  $\mathbf{b}$  may significantly deviate from the true state of the system  $\mathbf{x}$ , shown in Figure 1 and Figure 6.

The algorithm described in this paper is able to synthesize competitive emergent behavior such as blocking of other vehicles and cutting in front of others, illustrated in Figure 6. Additionally, although tight racing lines cut corners very closely, the chance constraints are successful in prohibiting

TABLE II  
RACING PERFORMANCE: DG VS MPC AND BSP VS NON-BSP

Competition Pair	Fraction of Fast winning
Fast DG BSP vs Slow MPC BSP	<b>82%</b>
Fast MPC BSP vs Slow DG BSP	<b>64%</b>
Fast DG BSP vs Slow DG non-BSP	<b>77%</b>
Fast DG non-BSP vs Slow DG BSP	<b>63%</b>

TABLE III  
RACING PERFORMANCE: WINNING RATIO

Competition Pair	Win ratio
DG BSP vs MPC BSP	<b>1.44:1</b>
DG BSP vs DG non-BSP	<b>1.33:1</b>

collisions under the presence of motion and observation noise.

2) *Benefits of Dynamic Game Planning:* We compare the performance of Dynamic Game (DG) planning to conventional methods such as Model Predictive Control (MPC). The MPC agent has the exact same cost structure, but assumes constant input of the other agent. Both DG and MPC plan in belief space. The MPC is capable of synthesizing competitive racing trajectories, shown in Figure 7, which are identical to the DG trajectories when no other agents are present. The performance of the DG planning distinguishes itself when interactions occur. We encourage interaction by starting one agent with lower drag coefficient (and therefore higher speed) behind another slower agent. The faster agent will eventually catch up to the previous agent and initiate an overtaking maneuver. The better interactions are predicted and integrated into planning, the more successful overtaking maneuvers will occur.

The results of 200 runs are displayed in Figure 7, Table II and Table III. The DG method wins 44% more races relative to the MPC baseline and has a larger lead on average. These results clearly illustrate the competitive advantage of our game-theoretic algorithm from leveraging how others react to one's own actions when planning.

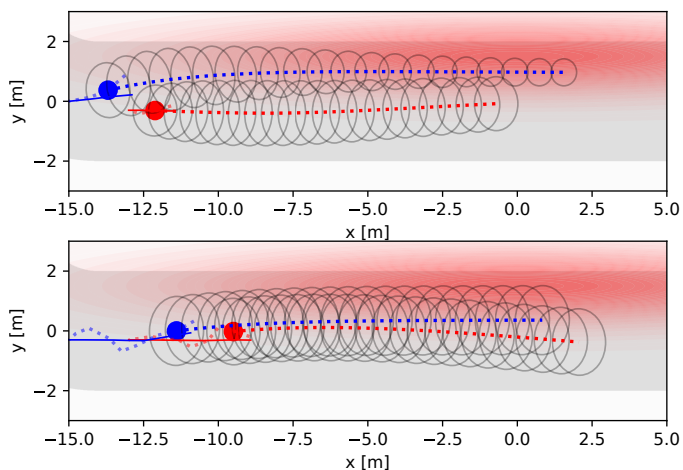


Fig. 8. **Top:** The blue agent overtakes the red agent by decreasing the uncertainty through the low noise region and reducing the chance constraint (ellipses). **Bottom:** The blue agent has the same uncertainty over the planning horizon and fails to overtake since the chance constraints remain large.

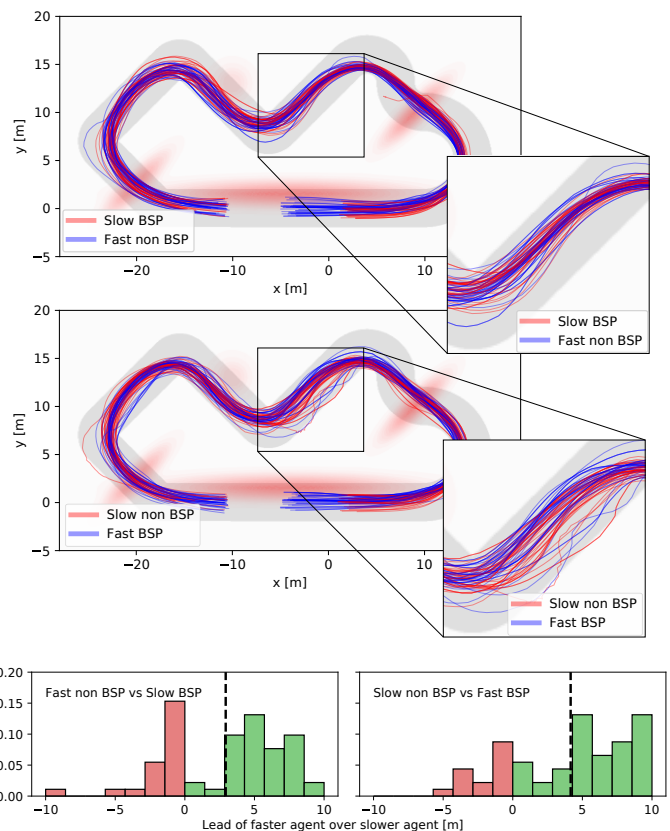


Fig. 9. **Top:** Traces of agents comparing BSP and non-BSP. In both cases the non BSP method shows more unsafe behavior, leaving the track several times and nearly colliding with the other agent. The BSP agent attempts more aggressive overtaking maneuvers due to the lower uncertainty estimate over itself and the other agent, as shown in the cutout. **Bottom:** Histograms of the  $\Delta$ arc-length lead of the faster agent over the slower agent. Here, the BSP method won more races than the non-BSP method and had a higher average lead.

3) *Benefits of Belief Space Planning:* We also compare the performance of DG planning with and without Belief Space Planning (BSP). In the non-BSP case the current belief  $\mathbf{b}_0$  is held constant over the planning horizon instead of being influenced by expected measurements. Note that the current belief is still updated online by an EKF for both agents. Results are reported in Figure 9 and Table II. The BSP variant wins 33% more races, has a larger average lead, and the fewest number of collisions. The non-BSP method collides nearly 10 times more often and exhibits behavior inappropriate for observed uncertainty levels, such as being too conservative because low noise regions are not considered in the planning phase, or too aggressive when entering sharp turns since additional sensor noise due to breaking and steering are not accounted for.

Figure 8 gives an intuitive explanation for the competitive advantage of planning in belief space. Without information gain, the follower will never be able to overtake due to the large chance constraint, whereas with information gain, the chance constraint shrinks while moving through a low noise zone, allowing the blue agent to overtake the leading agent. As shown in Figure 9 the BSP agent is able to adapt their trajectories to account for increased noise due to strong

actuation, i.e. braking and steering, and gaining information in low noise regions.

#### D. Real-Time Implementation Details

We implement our solver in the CasADi [34] framework leveraging auto-differentiation by source code transformation, automatic problem specific compute graph generation, C-code generation, and sparse operations. Exploiting sparsity is highly important to allow for real-time performance since the belief space, encompassing the mean state and the upper triangle of the covariance matrix can make respective Jacobian and Hessian matrices very large. The average compute times on a Ryzen 7 1700X 3.4 GHz are reported in Table IV. Algorithm 1 was run until convergence starting from a cold start for all experiments, i.e. the initial control trajectory  $\mathbf{u}$  consists of all zeros. Nonetheless, it is also possible to run the algorithm sequentially by hot starting the optimization with the previous solution. This is common practice in related optimization techniques for controls such as sequential quadratic programming [35] and allows to run Algorithm 1 at 100-200Hz. In these cases it is often enough to run only very few iterations to update the previous solution.

TABLE IV  
AVERAGE COMPUTATION TIME

Experiment	Per iteration	Until convergence
Active surveillance	9.3 ms	371.3 ms
Guide dog	11.2 ms	474.9 ms
Racing	5.8 ms	110.5 ms

#### V. CONCLUSIONS

In this paper, we propose a formulation for integrating belief space planning into dynamic games, and present a real-time algorithm for solving the local Nash equilibria of these dynamic games in belief space. We demonstrate its performance of combining game-theoretic planning and information gathering with three case studies: active surveillance, guiding blind agents, and racing with autonomous vehicles.

While game-theoretic planning models the interaction and dependency among agents, it does not address the quality of information available to the agent for decision making. Incorporating belief space planning in dynamic games allows for new capabilities not possible with other approaches, essential in house service robots or interacting with human agents in traffic. Reasoning about another agent’s uncertainty and simultaneously leveraging the effect of own actions on other agents’ actions results in complex emergent behavior such as indirectly pushing and guiding others through regions of light, without the use of any form direct of communication.

In competitive use cases such as racing emergent behavior consists of cutting, blocking, forcing others to break hard with the goal of increasing their uncertainty and slowing them down in turns, as well as the exploitation of high information-gain zones for overtaking. In particular, game-theoretic belief space planning significantly increased performance in dynamic racing when benchmarked against state-of-the-art

planning methods. Game-theoretic belief space planning wins 44% more races when competing with a non-game-theoretic baseline with belief space planning and 34% more races than a game-theoretic baseline without belief space planning. In this work we limit ourselves to first-order beliefs to avoid the explosion in parameters for recursive beliefs over beliefs. Nonetheless, even in cases where a first-order belief assumption is a simplification of the true belief dynamics, such as racing, we see improved performance to baselines that do not take the belief over other agents into account. In future work we would like to develop extensions beyond first-order belief spaces.

We achieve real-time performance running our algorithm at 100Hz, efficiently solving for a Nash equilibrium in belief space, by solving a quadratic game at each stage of the recursive backward pass of a belief space variant of iLQG. This results in linear complexity in the planning horizon in comparison to exponential complexity of point-based POMDP algorithms.

#### REFERENCES

- [1] B. D. Ziebart, A. Maas, J. A. Bagnell, and A. K. Dey, “Maximum entropy inverse reinforcement learning,” 2008.
- [2] D. Sadigh, S. Sastry, S. A. Seshia, and A. D. Dragan, “Planning for autonomous cars that leverage effects on human actions.”
- [3] M. Kuderer, S. Gulati, and W. Burgard, “Learning driving styles for autonomous vehicles from demonstration,” in *2015 IEEE International Conference on Robotics and Automation (ICRA)*. IEEE, 2015, pp. 2641–2646.
- [4] H. Kretzschmar, M. Kuderer, and W. Burgard, “Learning to predict trajectories of cooperatively navigating agents,” in *2014 IEEE international conference on robotics and automation (ICRA)*. IEEE, 2014, pp. 4015–4020.
- [5] N. Li, D. W. Oyler, M. Zhang, Y. Yildiz, I. Kolmanovsky, and A. R. Girard, “Game theoretic modeling of driver and vehicle interactions for verification and validation of autonomous vehicle control systems,” *IEEE Transactions on control systems technology*, vol. 26, no. 5, pp. 1782–1797, 2018.
- [6] W. Schwarting, A. Pierson, S. Karaman, and D. Rus, “Social behavior for autonomous vehicles,” *submitted*, 2019.
- [7] W. Schwarting, J. Alonso-Mora, and D. Rus, “Planning and decision-making for autonomous vehicles,” *Annual Review of Control, Robotics, and Autonomous Systems*, vol. 1, pp. 187–210, 2018.
- [8] J. R. Marden and J. S. Shamma, “Game theory and control,” *Annual Review of Control, Robotics, and Autonomous Systems*, no. 0, 2018.
- [9] G. Williams, B. Goldfain, P. Drews, J. M. Rehg, and E. A. Theodorou, “Best response model predictive control for agile interactions between autonomous ground vehicles,” in *2018 IEEE International Conference on Robotics and Automation (ICRA)*. IEEE, 2018, pp. 2403–2410.

- [10] A. Liniger and J. Lygeros, “A non-cooperative game approach to autonomous racing,” *arXiv preprint arXiv:1712.03913*, 2017.
- [11] R. Spica, D. Falanga, E. Cristofalo, E. Montijano, D. Scaramuzza, and M. Schwager, “A real-time game theoretic planner for autonomous two-player drone racing,” in *2018 Robotics Science and Systems (RSS)*, 1801.
- [12] A. Dreves and M. Gerdtts, “A generalized nash equilibrium approach for optimal control problems of autonomous cars,” *Optimal Control Applications and Methods*, vol. 39, no. 1, pp. 326–342, 2018.
- [13] L. P. Kaelbling, M. L. Littman, and A. R. Cassandra, “Planning and acting in partially observable stochastic domains,” *Artificial intelligence*, vol. 101, no. 1-2, pp. 99–134, 1998.
- [14] H. Bai, D. Hsu, and W. S. Lee, “Integrated perception and planning in the continuous space: A pomdp approach,” *The International Journal of Robotics Research*, vol. 33, no. 9, pp. 1288–1302, 2014.
- [15] H. Kurniawati, D. Hsu, and W. S. Lee, “Sarsop: Efficient point-based pomdp planning by approximating optimally reachable belief spaces.” in *Robotics: Science and systems*, vol. 2008. Zurich, Switzerland., 2008.
- [16] J. Pineau, G. Gordon, S. Thrun *et al.*, “Point-based value iteration: An anytime algorithm for pomdps,” in *IJCAI*, vol. 3, 2003, pp. 1025–1032.
- [17] E. A. Hansen, D. S. Bernstein, and S. Zilberstein, “Dynamic programming for partially observable stochastic games,” in *AAAI*, vol. 4, 2004, pp. 709–715.
- [18] A. Bry and N. Roy, “Rapidly-exploring random belief trees for motion planning under uncertainty,” in *Robotics and Automation (ICRA), 2011 IEEE International Conference on*. IEEE, 2011, pp. 723–730.
- [19] S. Patil, J. Van Den Berg, and R. Alterovitz, “Estimating probability of collision for safe motion planning under gaussian motion and sensing uncertainty,” in *Robotics and Automation (ICRA), 2012 IEEE International Conference on*. IEEE, 2012, pp. 3238–3244.
- [20] S. Prentice and N. Roy, “The belief roadmap: Efficient planning in belief space by factoring the covariance,” *The International Journal of Robotics Research*, vol. 28, no. 11-12, pp. 1448–1465, 2009.
- [21] A. Lee, Y. Duan, S. Patil, J. Schulman, Z. McCarthy, J. van den Berg, K. Goldberg, and P. Abbeel, “Sigma hulls for gaussian belief space planning for imprecise articulated robots amid obstacles,” in *Intelligent Robots and Systems (IROS), 2013 IEEE/RSJ International Conference on*. IEEE, 2013, pp. 5660–5667.
- [22] S. Patil, G. Kahn, M. Laskey, J. Schulman, K. Goldberg, and P. Abbeel, “Scaling up gaussian belief space planning through covariance-free trajectory optimization and automatic differentiation,” in *Algorithmic foundations of robotics XI*. Springer, 2015, pp. 515–533.
- [23] R. Platt, R. Tedrake, L. Kaelbling, and T. Lozano-Perez, “Belief space planning assuming maximum likelihood observations,” in *Robotics Science and Systems Conference (RSS)*, 2010.
- [24] J. Van Den Berg, S. Patil, and R. Alterovitz, “Motion planning under uncertainty using iterative local optimization in belief space,” *The International Journal of Robotics Research*, vol. 31, no. 11, pp. 1263–1278, 2012.
- [25] W. Sun, J. van den Berg, and R. Alterovitz, “Stochastic extended lqr for optimization-based motion planning under uncertainty,” *IEEE Transactions on Automation Science and Engineering*, vol. 13, no. 2, pp. 437–447, 2016.
- [26] B. Scassellati, “Theory of mind for a humanoid robot,” *Autonomous Robots*, vol. 12, no. 1, pp. 13–24, 2002.
- [27] S. Thrun, W. Burgard, and D. Fox, *Probabilistic robotics*. MIT press, 2005.
- [28] T. Basar and G. J. Olsder, *Dynamic noncooperative game theory*. Siam, 1999, vol. 23.
- [29] J. Van Den Berg, S. Patil, and R. Alterovitz, “Motion planning under uncertainty using iterative local optimization in belief space,” *The International Journal of Robotics Research*, vol. 31, no. 11, pp. 1263–1278, 2012.
- [30] E. Wan, “Sigma-point filters: An overview with applications to integrated navigation and vision assisted control,” in *Nonlinear Statistical Signal Processing Workshop, 2006 IEEE*. IEEE, 2006, pp. 201–202.
- [31] S. J. Julier and J. K. Uhlmann, “Unscented filtering and nonlinear estimation,” *Proceedings of the IEEE*, vol. 92, no. 3, pp. 401–422, 2004.
- [32] K. Levenberg, “A method for the solution of certain nonlinear problems in least squares,” *Quarterly of applied mathematics*, vol. 2, no. 2, pp. 164–168, 1944.
- [33] Y. Tassa, T. Erez, and E. Todorov, “Synthesis and stabilization of complex behaviors through online trajectory optimization,” in *Intelligent Robots and Systems (IROS), 2012 IEEE/RSJ International Conference on*. IEEE, 2012, pp. 4906–4913.
- [34] J. A. E. Andersson, J. Gillis, G. Horn, J. B. Rawlings, and M. Diehl, “CasADi – A software framework for nonlinear optimization and optimal control,” *Mathematical Programming Computation*, In Press, 2018.
- [35] J. Nocedal and S. Wright, *Numerical optimization*. Springer Science & Business Media, 2006.